Macromolecules

ARTICLE

pubs.acs.org/Macromolecules

Mechanical Reinforcement in Polymer Melts Filled with Polymer Grafted Nanoparticles

Joseph F. Moll,[†] Pinar Akcora,[‡] Atri Rungta,[§] Shushan Gong,[⊥] Ralph H. Colby,[⊥] Brian C. Benicewicz,[§] and Sanat K. Kumar*[,‡]

[†]Department of Chemistry, Columbia University, 5000 Broadway, New York, New York 10027, United States

[‡]Department of Chemical Engineering, Columbia University, 500 W. 120th St., New York, New York 10027, United States

[§]Department of Chemistry and Biochemistry, University of South Carolina, Columbia, South Carolina 29208, United States

[⊥]Department of Material Science and Engineering, Pennsylvania State University, University Park, Pennsylvania 16802, United States

ABSTRACT: We critically leverage the fact that polymer grafted nanoparticles behave akin to block copolymers to systematically vary nanoparticle dispersion and critically examine its role on the mechanical reinforcement in liquid-polymer-based nanocomposites. The nanoparticles are noncontacting, and we perform rheological measurements 80K above the polymer's glass transition temperature. Our rheology results unequivocally show that reinforcement is maximized by the formation of a transient, but long-lived, percolating polymer−particle network with the particles serving as the network junctions.

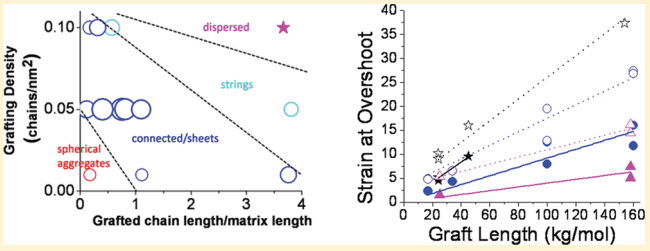

I. INTRODUCTION

The addition of filler has been found to dramatically enhance the mechanical properties of polymeric materials.[1] The mechanism of reinforcement, however, remains in debate, and there are three scenarios that have been proposed. At one extreme, mechanical reinforcement is suggested to be due to the agglomeration of particles; when these agglomerates percolate through the system, then, there is a direct pathway for the propagation of stress and hence mechanical reinforcement.[1−4] In contrast to this "particle-only" scenario, others involve both the particles and polymer chains. Long et al.[5] used the fact that chain immobilization occurs around nanoparticles[6]—they suggested that mechanical reinforcement is found when the particles with the "bound" glassy layers percolate.[7−10] A final scenario proposed by Goritz,[11] and elaborated upon by Wang[12] and Sternstein,[13] is that the particles form a network, with the polymer chains forming the "bridges" between the particles.

Crucial to resolving this argument is the ability to control the nanofiller dispersion state. Particularly relevant is that we previously showed that silica nanoparticles uniformly grafted with polystyrene behaved akin to block copolymers because of the dislike between the silica cores and the polystyrene corona. These grafted particles thus self-assembled into a variety of anisotropic structures when they were placed in a polystyrene matrix (Figure 1).[14] We have used this ability to examine the mechanical behavior of nanocomposites at two extremes of particle dispersion, i.e., well-dispersed particles vs particles self-assembled into percolating structures.[15] Since the latter case yielded mechanical reinforcement at a much lower particle loading than the former, mechanical reinforcement appears to be primarily controlled by interparticle interactions (including those facilitated by the grafted chains), and the matrix polystyrene plays a relatively minor role. While this picture lends some clarity to the origins of mechanical reinforcement, the role of the polymer is not resolved. If it does play a role, then does the scenario of Long et al. or the Goritz picture have more relevance? Answering this underpinning question is the focus of this paper.

II. EXPERIMENTAL SECTION

Polystyrene chains are grown from the surfaces of spherical silica nanoparticles (diameter = 14 ± 4 nm, Nissan Chemicals) using reversible addition−fragmentation chain transfer (RAFT) polymerization.[16−19] The chain length of the grafts and the graft densities are varied systematically in a series of samples.[14,20] The grafted particles are dissolved in solvent, either benzene or tetrahydrofuran (THF), and mixed with a monodisperse polystyrene matrix dissolved in the same solvent. This solution is sonicated (2 s sonication, 1 s rest) for 3 min, poured into a 60 mm diameter Petri dish, dried overnight in a vacuum oven, and then annealed for 5 days at 10^{-4} Torr at 150 °C. All the composites have 5 wt % of the silica core unless otherwise noted. The samples are analyzed by transmission electron microscopy (TEM), USAXS (not reported here), and rheology. TEM samples are microtomed (thickness ∼60 nm) and transferred to a Formvar-coated copper TEM grid.

Rheological samples are dried for 5 days at 80 °C to remove any solvent and molded into cylindrical discs 1−2 mm in thickness and 8 mm in diameter. Samples for the start-up of steady shear at various

Received: May 26, 2011
Revised: August 2, 2011
Published: August 24, 2011

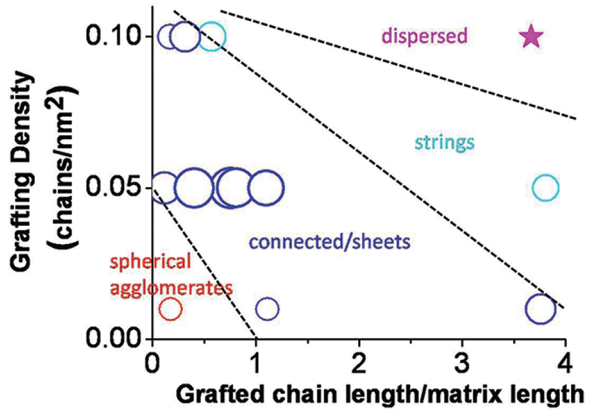

Figure 1. In a "morphology" diagram we plot symbols whose size scale with the degree of reinforcement as characterized by the ratio stress overshoot maximum value/plateau value. Other measures give qualitatively similar results. Only the well-dispersed sample yielded no stress maximum.

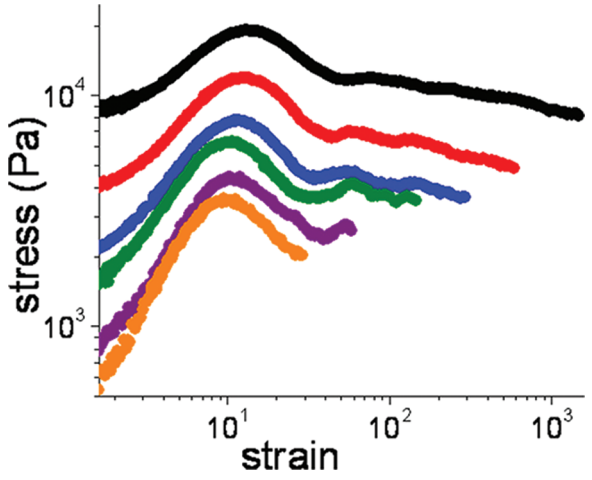

Figure 2. Strain of the shear stress overshoot is roughly independent of shear rate in the start-up of steady shear at 180 °C. The sample was sheared at six different rates: 0.5 (black), 0.2 (blue), 0.1 (red), 0.05 (green), 0.02 (purple), and 0.01 (orange) (s^{-1}). The grafted chain length is 100 kg/mol, the grafting density is 0.05 chains/nm^2, and the matrix chain length is 132.9 kg/mol. Electron micrographs confirm a connected nanoparticle network.

rates are carefully treated in precisely the same fashion for annealing, molding, and loading into the rheometer to facilitate comparison. All rheological measurements are made at 180 °C.

III. RESULTS AND DISCUSSION

We have used both linear oscillatory shear and "start-up" of steady shear experiments to study a range of nanocomposites.[14,20] Start-up of steady shear experiments at a variety of strain rates (0.01−0.5 s^{-1}) show the same qualitative behavior—e.g., we observe a stress maximum as a function of time with the strain value at the stress maximum decreasing slightly with decreasing strain rate (Figure 2). Similar results have been previously reported,[21] in agreement with the notion that this stress maximum, which is a manifestation of the transient elastic (or solid-like) behavior of the reinforced samples, must disappear in the limit of zero strain rate. Flow reversal experiments were performed to determine whether the overshoot is recoverable; samples that had been sheared past the stress maximum at a shear rate of 0.2 s^{-1} were reannealed for 1 week at 150 °C. These samples displayed an overshoot.

Of 13 nanocomposites studied only the sample with well-dispersed nanoparticles shows no overshoot. Our past work has shown that the well-dispersed sample will also show solidlike behavior, but at higher particle concentration (∼15 wt % silica).[15] TEM micrographs are shown for three distinct dispersion states (agglomerated clusters, a connected nanoparticle network, and sheets) in Figure 3a. The dimensionality of these structures was determined by comparing consecutive microtomed slices of sample.[14] The grafted chain length to matrix chain length ratio was held roughly constant, and the grafting density was varied in the range 0.01−0.1 chains/nm^2. Start-up of steady shear experiments (Figure 3b) display a stress overshoot in each case, although the peak is small in the nanocomposite with small particle agglomerates. A maximum in stress overshoot is seen for the intermediate graft density. These results are corroborated by linear oscillatory shear experiments, which show that this intermediate grafting density also has the most reinforcement, as evidenced by the height of the low-frequency modulus in Figure 3c. Thus, the reinforcement is strongly correlated to the nanoparticle morphology, with an apparent maximum being obtained when the particle structures percolate. This is in line with the expectations of Payne, Gusev, and many other past works, including our own.[21−23]

To critically resolve the role of the polymer matrix, it is important to consider samples across the whole morphology diagram (Figure 1). A difficulty is that the matrix polymer molecular weight has to be varied to achieve the desired broad range of the ratio of the graft length to matrix length. Since there is a strong dependence of the absolute values of the modulus on the matrix molecular weight, we need a measure of mechanical reinforcement that normalizes out this variable. We found that the stress value at the peak of the overshoot scaled by the stress plateau value at large strain (long time) is particularly appropriate, as utilized previously.[21,24] This analysis (Figure 1 and Table 1) shows that, as expected, the largest reinforcement occurs in the regions corresponding to networks of particles. Perhaps more interesting is the trend seen for various percolated samples, all with similar morphologies, but with widely varying graft densities—apparently, the reinforcement goes through a maximum at an intermediate graft density (0.05 chains/nm^2). This result offers a crucial insight—apparently, the grafted chains play a central role in reinforcement. Were a particle-only scenario operative, then, we should have maximum reinforcement in the limit of very low grafting densities, where the particle cores could contact other cores. We elaborate on this point below.

More insight into the mechanism of reinforcement, specifically, the role of graft chains, results when we plot the strain value at both the shear stress (σ) maximum and the primary normal stress (N_1) maximum as a function of graft chain length (Figure 4). We plot N_1 along with σ because it displays a maximum in all filled samples, even in cases where the dispersion state does not allow for a nanoparticle network to span the material (and thus we see no shear stress maximum). The observed strong linear correlation in this figure implies that the stress maximum is driven by the existence of a particle network, where the network "connectivity" is transmitted by the grafted chains. Thus, while the dispersion state of the filler is primarily responsible for the magnitude of reinforcement, the presence of the grafted chains enhances

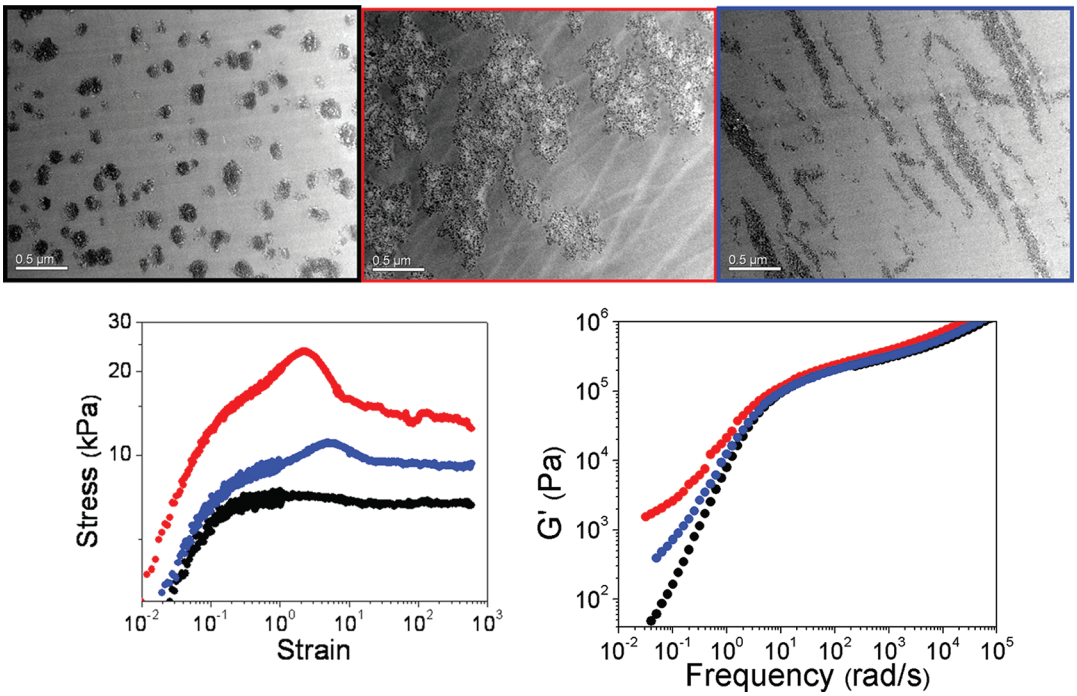

Figure 3. (A) TEM images showing nanoparticle dispersion states. All three samples have a 142 kg/mol matrix. Left: agglomerated, 25 kg/mol graft, 0.01 chains/nm^2 (black). Center: a particle network, 17 kg/mol graft, 0.05 chains/nm^2 (red). Right: sheets of particles, 24 kg/mol graft, 0.1 chains/nm^2 (blue). (B) Steady shear data at 180 °C at a shear rate of 0.2/s. (C) Storage modulus data for the same three nanocomposites, also taken at 180 °C.

Table 1. Reinforcement Metric (Stress Value at the Peak of the Overshoot Scaled by the Large Strain Stress Plateau)[a]

matrix M_n (kg/mol)	matrix PDI	graft M_n (kg/mol)	graft density (chains/nm^2)	graft PDI	morphology	overshoot/plateau
142	1.04	160	0.05	1.21	connected	1.36
142	1.04	158	0.01	1.5	sheets	1.07
142	1.04	45	0.1	1.06	connected	1.38
142	1.04	25	0.01	1.2	aggregates	1.08
142	1.04	24	0.1	1.04	sheets	1.17
142	1.04	17	0.05	1.05	connected	1.48
131.4	1.01	100	0.05	1.2	connected	1.83
42.2	1.04	160	0.05	1.21	strings	1.23
42.2	1.04	158	0.01	1.5	connected	1.40
42.2	1.04	154	0.1	1.25	dispersed	no overshoot
42.2	1.04	34	0.05	1.05	connected	1.81
42.2	1.04	24	0.1	1.04	connected	1.35
42.2	1.04	17	0.05	1.05	connected	1.82

[a] The highest reinforcement occurs in the morphologies with a connected nanoparticle network.

this effect. Apparently, this increases the strain to "break" the particle network, which we believe to be the origin of the stress maximum.

We now ask why the stress maximum is optimized only at an intermediate graft density and why both lower and higher graft densities show lower reinforcement. For extremely low graft densities, there are very few graft chains—since we postulate that the "interaction" of graft chains is crucial, it then follows that low graft densities do not offer substantial reinforcement. The reduction of reinforcement at high graft densities is attributed to the particular shape of the morphology diagram (Figure 1)—as one increases the graft density, the x-axis values have to get smaller to maintain a given morphology (in this case particle morphologies which percolate). Consider a fixed matrix molecular weight—this implies that the graft chain length must decrease as graft chain density increases to maintain the same morphology. Since the extent of the interaction between grafted chains is expected to decrease with decreasing graft length, then it follows that the stress reinforcement must eventually decrease with increasing graft density for a given particle morphology. For 14 nm silica at 5 wt %, the typical spacing between particles is ~50 nm. The longest grafts with $M_n \approx 160$ kg/mol have size of ~20 nm, but at 0.01 chains/nm^2 there are only 6 grafted chains on each particle so they barely entangle, while at 0.05 chains/nm^2 there are 30 grafted chains on each particle and they entangle significantly. For grafting density 0.1 chains/nm^2 shorter grafts

dx.doi.org/10.1021/ma201200m |*Macromolecules* 2011, 44, 7473–7477

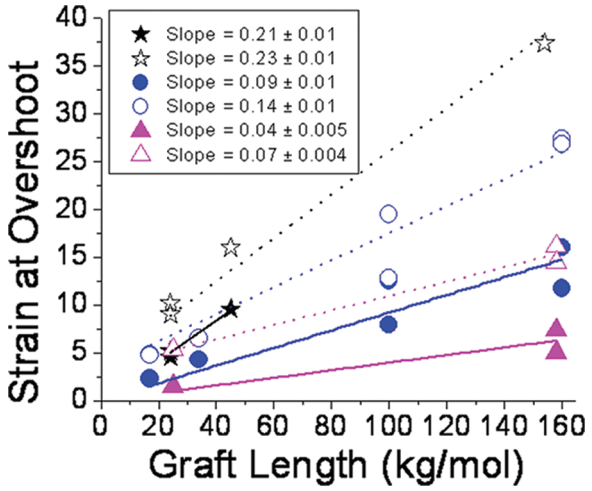

Figure 4. Deformation necessary for the shear stress overshoot increases linearly as a function of the grafted chain length. We consider three grafting densities: 0.1 chains/nm^2 (black stars), 0.05 chains/nm^2 (blue circles), and 0.01 chains/nm^2 (pink triangles). Both N_1 overshoot (open symbols) and σ overshoot strains (closed symbols) are displayed. The lines are simply guides to the eye.

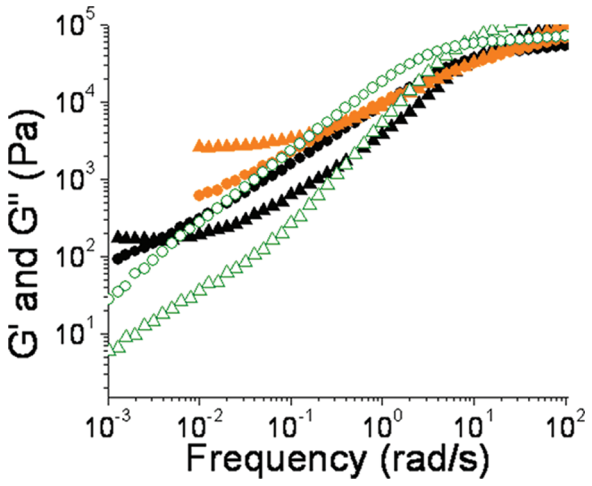

Figure 5. 180 °C storage moduli (triangles) and loss moduli (circles) at different loadings: 5% (open green), 8% (black), and 15% silica (gold). The graft molecular weights are 52, 114, and 150 kg/mol, respectively. Matrix molecular weight is 129.2 kg/mol for 5% and 8% particle loadings and 150 kg/mol for 15% silica.

with M_n < 50 kg/mol are used, and these have size smaller than 15 nm and cannot reach the grafts on other particles so they cannot form graft−graft entanglements. This result argues for the crucial role of graft chains in mechanical reinforcement.

This mechanical reinforcement can also be understood in the context of rubber elasticity theory. In Figure 5 we consider composites with 5, 8, and 15 wt % silica nanoparticles, from the region of our morphology diagram where we have observed the highest degree of mechanical reinforcement, i.e., percolating particles at an intermediate graft density of 0.05 chains/nm^2. If we extrapolate our low-frequency plateau in G' (the equilibrium modulus of the nanoparticle network G_{eq}) down to a modulus of zero by plotting $G_{eq}^{1/3}$ vs the wt % of silica, the onset of gelation is predicted to be ∼3.2 wt % silica and the modulus expected for the 5 wt % sample is 8 Pa (near the border of our lowest measurements). According to the phantom network model,[25] the number density of elastically effective network strands ν in excess of the number density of elastically effective junction points μ is $\nu - \mu = G_{eq}/k_BT$. We assume every particle acts as a network junction point, making $\mu = 5.2 \times 10^{16}$ particles/cm^3 for the 15 wt % and $\mu = 2.6 \times 10^{16}$ particles/cm^3 for the 8 wt %. Using the measured G_{eq} of 2610 and 172 Pa for the 15% and 8% composites, respectively, yields $\nu - \mu = 4.17 \times 10^{17}$ strands/cm^3 (9 graft−graft entanglements per particle) for the 15 wt % and 2.75×10^{16} strands/cm^3 (2 graft−graft entanglements per particle) for the 8 wt % nanocomposite. These data therefore support the picture that the mechanical reinforcement is driven primarily by the formation of a nanoparticle network, with the particles as the junction points and graft−graft entanglements as the elastically effective strands.

In this context, it appears that a glassy adsorbed polymer layer is not necessary to explain the observed reinforcement. Indeed, this mechanism for reinforcement is ruled out not only by the high temperature, T_g + 80 K, but also by the large distances between the particles. According to our previous work, well-dispersed particles at 15 wt % silica display an elastic modulus plateau,[15] suggesting reinforcement. In this well-dispersed system, the interparticle distance is ∼44 nm. Previous experimental work has suggested that the silica−polystyrene system is characterized by a bound (presumably glassy) layer of thickness ∼1 nm.[26] Given the particle size of 14 nm and the large interparticle spacing, we conclude that a bridging of glassy layers cannot explain our findings.

Jouaut et al.[27] studied bare silica particles in PS at very low percent silica. They discovered evidence of reinforcement in the existence of high temperature G' plateaus. These authors also rule out an overlap of glassy layers and suggest that the polystyrene matrix may be bridging particles, allowing interparticle interactions far below the volume fractions at which all of the nanoparticles contact each other. While the differences in the two systems make it difficult to directly compare, we posit that in cases such as these their adsorbed polymers are acting analogously to our chemically grafted polymers.

Furthermore, we emphasize that these tests were performed well above T_g and on a system of noncontacting nanoparticles, and thus other mechanisms of reinforcement may exist in different nanocomposite systems. However, our experimental system was chosen because of its relevance to industrial problems and specifically the optimal dispersion state of nanoparticles in automobile tires. By studying well above T_g and without cross-links, we are able to isolate the nanoparticle network, and it is the mechanism of reinforcement in this network that we address.

Our ability to systematically vary the nanoparticle morphology allows us to critically examine the factors that have been proposed to underlie mechanical reinforcement in polymer nanocomposites far above T_g. We show that the percolation of nanoparticles is necessary for stress propagation across the system—however, entanglement of grafted chains on different particles allows this percolation at lower particle loadings. Thus, our results unequivocally show that mechanical reinforcement here results from the formation of a network where the nanoparticles are the network junctions,[11,13,28−30] connected by graft−graft entanglements as the elastically effective network strands.

AUTHOR INFORMATION

Corresponding Author
*E-mail sk2794@columbia.edu; Ph (212)854-2193.

ACKNOWLEDGMENT

The authors acknowledge the extensive use of a ARES rheometer at the City College of New York. In particular, we thank Prof. Jeff Morris for access to this intrument. Financial support from NSF (DMR-0864847) is also gratefully acknowledged.

REFERENCES

(1) Payne, A. R. Effect of dispersion on the dynamic properties of filler-loaded rubbers. *J. Appl. Polym. Sci.* **1965**, *9*, 2273–2284.
(2) Payne, A. R. A note on the conductivity and modulus of carbon black-loaded rubbers. *J. Appl. Polym. Sci.* **1965**, *9*, 1073–1082.
(3) Heinrich, G.; Klüppel, M. Recent Advances in the Theory of Filler Networking in Elastomers. *Adv. Polym. Sci.* **2002**, *160*, 1–44.
(4) Gusev, A. A. Micromechanical Mechanism of Reinforcement and Losses in Filled Rubbers. *Macromolecules* **2006**, *39* (18), 5960–5962.
(5) Long, D.; Sotta, P. Stress relaxation of large amplitudes and long timescales in soft thermoplastic and filled elastomers. *Rheol. Acta* **2007**, *46* (8), 1029–1044.
(6) Vondracek, P.; Schatz, M. Bound Rubber and Crepe Hardening in Silicone-Rubber. *J. Appl. Polym. Sci.* **1977**, *21* (12), 3211–3222.
(7) Tsagaropoulos, G.; Eisenberg, A. Dynamic mechanical study of the factors affecting the two glass transition behavior of filled polymers. Similarities and differences with random ionomers. *Macromolecules* **1995**, *28* (18), 6067–6077.
(8) Bogoslovov, R. B.; Roland, C. M.; Ellis, A. R.; Randall, A. M.; Robertson, C. G. Effect of silica nanoparticles on the local segmental dynamics in poly(vinyl acetate). *Macromolecules* **2008**, *41* (4), 1289–1296.
(9) Sakai, V. G.; Arbe, A. Quasielastic neutron scattering in soft matter. *Curr. Opin. Colloid Interface Sci.* **2009**, *14* (6), 381–390.
(10) Gagliardi, S.; Arrighi, V.; Ferguson, R.; Telling, M. T. F. Restricted dynamics in polymer-filler systems. *Physica B: Condens. Matter* **2001**, *301* (1−2), 110–114.
(11) Maier, P. G.; Goritz, D. Molecular interpretation of the Payne effect. *Kautsch. Gummi Kunstst.* **1996**, *49* (1), 18–21.
(12) Zhu, Z. Y.; Thompson, T.; Wang, S. Q.; von Meerwall, E. D.; Halasa, A. Investigating linear and nonlinear viscoelastic behavior using model silica-particle-filled polybutadiene. *Macromolecules* **2005**, *38* (21), 8816–8824.
(13) Zhu, A. J.; Sternstein, S. S. Nonlinear viscoelasticity of nanofilled polymers: interfaces, chain statistics and properties recovery kinetics. *Compos. Sci. Technol.* **2003**, *63* (8), 1113–1126.
(14) Akcora, P.; Liu, H.; Kumar, S. K.; Moll, J.; Li, Y.; Benicewicz, B. C.; Schadler, L. S.; Acehin, D.; Panagiotopoulos, A. Z.; Pryamitsyn, V.; Ganesan, V.; Ilavsky, J.; Thiyagarajan, P.; Colby, R. H.; Douglas, J. F. Anisotropic particle self-assembly in polymer nanocomposites. *Nature Mater.* **2009**, *8*, 354–359.
(15) Akcora, P.; Kumar, S. K.; Moll, J.; Lewis, S.; Schadler, L. S.; Li, Y.; Benicewicz, B. C.; Sandy, A.; Narayanan, S.; Ilavsky, J.; Thiyagarajan, P.; Colby, R. H.; Douglas, J. F. "Gel-like" Mechanical Reinforcement in Polymer Nanocomposite Melts. *Macromolecules* **2010**, *43* (2), 1003–1010.
(16) Li, C.; Han, J.; Ryu, C. Y.; Benicewicz, B. C. A versatile method to prepare RAFT agent anchored substrates and the preparation of PMMA grafted nanoparticles. *Macromolecules* **2006**, *39* (9), 3175–3183.
(17) Li, C. Z.; Benicewicz, B. C. Synthesis of well-defined polymer brushes grafted onto silica nanoparticles via surface reversible addition-fragmentation chain transfer polymerization. *Macromolecules* **2005**, *38* (14), 5929–5936.
(18) Li, Y.; Benicewicz, B. C. Functionalization of Silica Nanoparticles via the Combination of Surface-Initiated RAFT Polymerization and Click Reactions. *Macromolecules* **2008**, *41* (21), 7986–7992.
(19) Schadler, L. S.; Kumar, S. K.; Benicewicz, B. C.; Lewis, S. L.; Harton, S. E. Designed interfaces in polymer nanocomposites: A fundamental viewpoint. *MRS Bull.* **2007**, *32* (4), 335–340.
(20) Samples not included in ref 14 are as follows: (1) 134 kg/mol matrix (PDI = 1.01), 100 kg/mol graft (PDI =1.2), 0.05 chains/nm^2; (2) 97 kg/mol matrix (PDI = 1.03), 100 kg/mol graft (PDI = 1.1), 0.05 chains/nm^2; (3) 129.2 kg/mol matrix (PDI =1.03), 52 kg/mol graft (PDI = 1.07), 0.05 chains/nm^2; (4) 129.2 kg/mol matrix (PDI = 1.03), 114 kg/mol graft (PDI = 1.07), 0.05 chains/nm^2.
(21) Solomon, M. J.; Almusallam, A. S.; Seefeldt, K. F.; Somwangthanaroj, A.; Varadan, P. Rheology of Polypropylene/Clay Hybrid Materials. *Macromolecules* **2001**, *34* (6), 1864–1872.
(22) Chatterjee, T.; Krishnamoorti, R. Dynamic consequences of the fractal network of nanotube-poly(ethylene oxide) nanocomposites. *Phys. Rev. E* **2007**, *75* (5).
(23) Goel, V.; Chatterjee, T.; Bombalski, L.; Yurekli, K.; Matyjaszewski, K.; Krishnamoorti, R. Viscoelastic properties of silica-grafted poly(styrene-acrylonitrile) nanocomposites. *J. Polym. Sci., Polym. Phys.* **2006**, *44* (14), 2014–2023.
(24) Treece, M. A.; Oberhauser, J. P. Soft glassy dynamics in polypropylene-clay nanocomposites. *Macromolecules* **2007**, *40* (3), 571–582.
(25) Staverman, A. J. Properties of phantom networks and real networks. *Adv. Polym. Sci.* **1982**, *44*, 73–101.
(26) Harton, S. E.; Kumar, S. K.; Yang, H. C.; Koga, T.; Hicks, K.; Lee, H. K.; Mijovic, J.; Liu, M.; Vallery, R. S.; Gidley, D. W. Immobilized polymer layers on spherical nanoparticles. *Macromolecules* **2010**, *43* (7), 3415–3421.
(27) Jouault, N.; Vallat, P.; Dalmas, F.; Said, S.; Jestin, J.; Boué, F. Well-dispersed fractal aggregates as filler in polymer-silica nanocomposites: long-range effects in rheology. *Macromolecules* **2009**, *42* (6), 2031–2040.
(28) Sternstein, S. S.; Ramorino, G.; Jiang, B.; Zhu, A. J. Reinforcement and nonlinear viscoelasticity of polymer melts containing mixtures of nanofillers. *Rubber Chem. Technol.* **2005**, *78* (2), 258–270.
(29) Sternstein, S. S.; Zhu, A. J. Reinforcement mechanism of nanofilled polymer melts as elucidated by nonlinear viscoelastic behavior. *Macromolecules* **2002**, *35* (19), 7262–7273.
(30) Salaniwal, S.; Kumar, S. K.; Douglas, J. F. Amorphous solidification in polymer-platelet nanocomposites. *Phys. Rev. Lett.* **2002**, *89*, 258301.